JOURNAL OF GEOPHYSICAL RESEARCH, VOL. 105, NO. E8, PAGES 20,403–20,415, AUGUST 25, 2000

The materials of the lunar Procellarum KREEP Terrane: A synthesis of data from geomorphological mapping, remote sensing, and sample analyses

Larry A. Haskin, Jeffrey J. Gillis, Randy L. Korotev, and Bradley L. Jolliff

Department of Earth and Planetary Sciences and McDonnell Center for the Space Sciences
Washington University, St. Louis, Missouri

Abstract. Major features of the Moon's Procellarum KREEP Terrane include subdued relief and extensive resurfacing with mare basalt, consistent with high concentrations of Th and other heat-producing elements at depth. We relate the chemistry of sampled materials to the geomorphology, Th surface concentrations determined by the Lunar Prospector (2° pixels), and FeO and TiO_2 concentrations derived from Clementine ultraviolet-visible spectral data. On the basis of geologic maps, each pixel was classified as mare, terra, or mixed. Near the periphery of the terrane, terra pixel compositions are relatively feldspathic; in the interior they mainly represent Imbrium basin rim or ejecta deposits and are mainly incompatible trace element rich norites and presumably represent materials from a thick section (tens of kilometers) of the pre-Imbrium crust of the terrane excavated by the Imbrium event. (Although Imbrium ejecta are the principal source of surface terra materials, the Imbrium event did not create the Th-rich Procellarum KREEP Terrane.) Broad, continuous expanses of mare pixels are observed, with little interruption from protruding terra or terra-penetrating craters. The mare-basalt-dominated regoliths of these areas have a wide range of TiO_2 concentrations (<1 – 15%) and higher Th concentrations (2 to 6+ ppm) than most sampled mare basalts. Traverse profiles show high Th over broad regions of highest FeO (>18%), leading to the conclusion that the high Th concentrations are in the mare basalts and are not present in the regoliths as terra-derived materials. Volcanic glasses and impact glasses of mare basalt composition collected from the Procellarum KREEP Terrane support this conclusion.

1. Introduction

In a companion paper [*Jolliff et al.*, 2000] we suggest that the traditional "mare-highland" dichotomy is no longer a useful classification of the lunar surface, given the new information we have obtained about the Moon from the Clementine and Lunar Prospector missions. Instead, we advocate that the Moon consists of three major terranes (i.e., major geochemical and geological provinces), the Procellarum KREEP Terrane, the Feldspathic Highlands Terrane, and the South Pole-Aitken Terrane. According to this view, maria are included as part of the terrane in which they occur. In Jolliff et al. we address general characteristics of the three major terranes, with some emphasis on Th concentrations derived from the Lunar Prospector gamma-ray spectrometer. Here we discuss the distribution of Th, FeO, and TiO_2 within the Procellarum KREEP Terrane in terms of the chemistry of the materials in the Apollo, Luna, and lunar meteorite collections and in the context of the regional morphological units as mapped photogeologically. We address these questions: 1) What are the materials of the Procellarum KREEP Terrane? 2) What is the relationship of these materials to the geomorphologic units of this terrane? 3) Is the Th enrichment of the Procellarum KREEP Terrane a consequence of deep Imbrium excavation into a global KREEP-rich (Potassium, Rare Earth Element, and Phosphorous) layer or inherent and unique to the terrane?

The Th map of the Procellarum KREEP Terrane (based on our calibration for the Th data; see the next section) is shown as Plate 1. As in the map of *Lawrence et al.* [1999], the most striking feature of the Th distribution map is the high Th concentrations, which are restricted almost entirely to the Mare Imbrium-Oceanus Procellarum region (the Procellarum KREEP Terrane). The Procellarum KREEP Terrane is the only major region of the Moon where Th, K, and, presumably, the other incompatible trace elements are generally enriched (2.2 – 13 ppm Th). Because of the nearly constant relative proportions of incompatible trace elements in most lunar polymict samples, we use Th in this paper as a proxy for KREEP. (KREEP is defined here as incompatible trace elements occurring in the relative abundances that are common in trace-element-rich lunar materials such as Apollo 14 mafic impact-melt breccias.) The highest Th concentrations (13 ppm) observed within the Procellarum KREEP Terrane (e.g., near the craters Aristillus and Aristarchus and in the Fra Mauro region) reach the Th concentration typical of Apollo 14 regolith. The general level of Th concentrations within the Procellarum KREEP Terrane is much higher than that of the South Pole-Aitken Terrane and the Feldspathic Highlands Terrane. The high Th concentrations of the Procellarum KREEP Terrane taper off gradually with distance outside of the Imbrium-Procellarum region to low concentrations across the rest of the Moon except for the somewhat raised concentrations within the South Pole-Aitken Basin (0 – 4.5 ppm, mostly <3 ppm) and a small area (60°N,

Paper number 1999JE001128.
0148-0227/00/1999JE001128$09.00

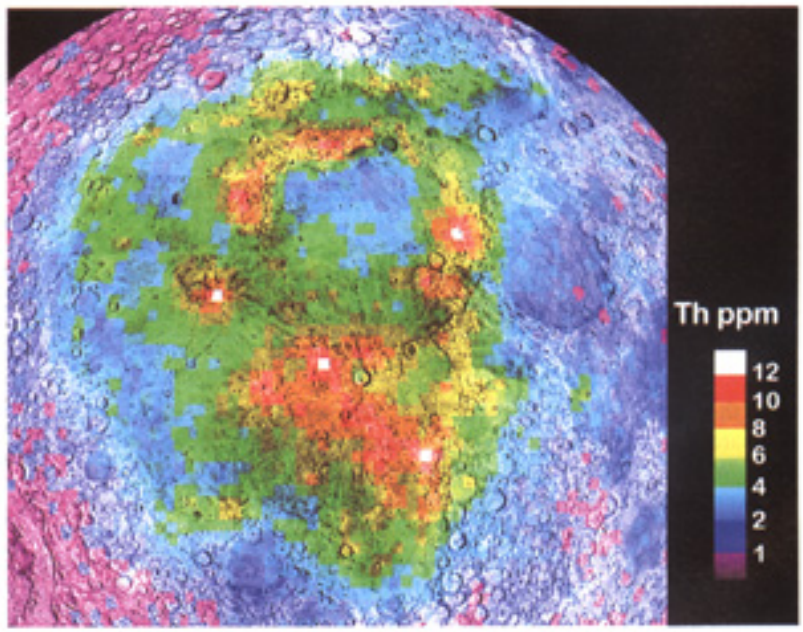

Plate 1. This map shows the distribution of Th within the Procellarum KREEP Terrane as determined using a ground-truth calibration. Here the Th map is merged with a shaded relief map to allow the association of morphologic with compositional features. The absolute Th abundance is based on total counts per 32 seconds in the spectral region of the main ^{232}Th γ-ray (2.61±0.1 MeV) [*Lawrence et al.*, 1999], and these counts have been corrected for gain, dead time, cosmic-ray variations, and asymmetric response of the instrument. The map is in a Lambert equal-area projection, extending from 120°W to 30°E and 90°S to 90°N and centered on 30°W.

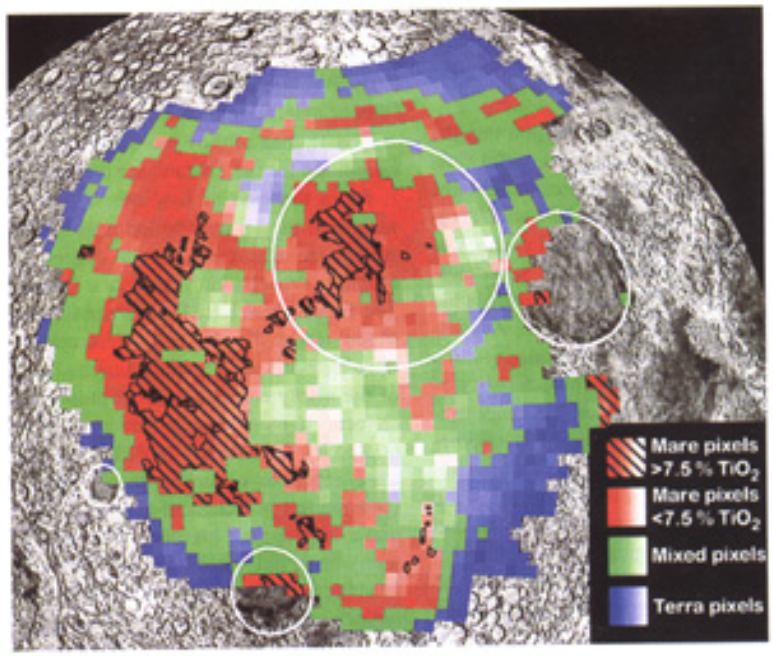

Plate 2. The spatial relationships among the three principal materials mapped in the Procellarum KREEP Terrane (mare, mixed, and terra) are illustrated in this map. The color of each pixel denotes the material (terra >90%, mare >90%, or mixed if a terra-mare boundary underlies the pixel). The intensity of the color within each pixel is controlled by Th concentration (whiter being higher Th). A hatched overlay shows the spatial distribution of mare basalt >7.5 wt% TiO_2; most of the basaltic plains underlying these higher-TiO_2 areas are Eratosthenian. The three white circles represent the Imbrium, Nubium, and Grimaldi basins in order of decreasing size. The map is in a Lambert equal-area projection, extending from 120°W to 30°E and 90°S to 90°N and centered on 30°W.

100°E) between the craters Belkovich (63°N, 90°E) and Compton (55°N, 105°E) (~10 ppm) [*Lawrence et al.*, 1999].

2. Data Classification and Calibration

For this work we use three principal data sets for concentrations of chemical elements: the Th data of *Lawrence et al.* [1999] obtained from the Lunar Prospector gamma-ray spectrometer [*Binder*, 1998], FeO and TiO_2 concentrations derived from the Clementine ultraviolet-visible (UVVIS) data [*Lucey et al.*, 1998, this issue], and average concentrations of Th, FeO, and TiO_2 in different classes of lunar samples [*Korotev*, 1998]. To relate element concentrations to geologic units, we use the maps of *Wilhelms and McCauley* [1971] and *Lucchitta* [1978].

2.1. Classification of Pixels

In order to examine the chemistry of the Procellarum KREEP Terrane in the context of the chemistry of the lunar samples, we have classified each equal-area pixel of the Th map of *Lawrence et al.* [1999] that falls within the Procellarum KREEP Terrane as terra, mare, or mixed on the basis of the geologic maps [*Wilhelms and McCauley*, 1971; *Lucchitta*, 1978]. To be classified as terra or mare, the mapped terrain under a pixel had to be ≥90% one or the other. Pixels that did not meet those criteria are classified as mixed. Of the 1926 pixels within the Procellarum KREEP Terrane, 18% are classified as terrae, 38% as maria, and 44% as mixed. The term "mixed" does not indicate regoliths with components from both mare and terra locations; it means that a boundary between mare and terra crosses the pixel. (All pixels

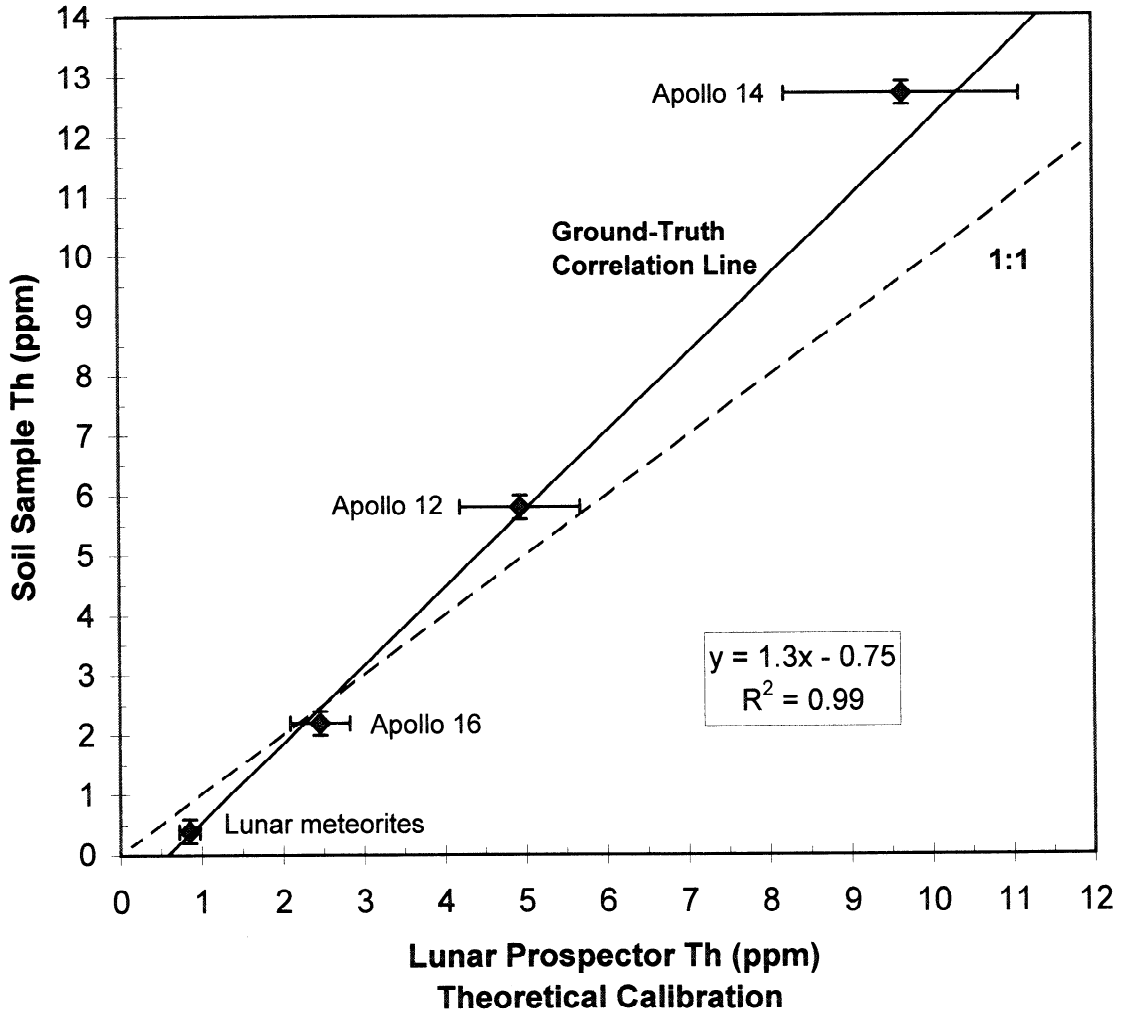

Figure 1. A comparison between Th abundances in soil samples from sites that are compositionally uniform at the 1° scale and pixels in the Prospector γ-ray data that cover these regions [*Lawrence et al.*, 1999]. For the feldspathic lunar meteorites [*Korotev*, 1999] we plot the median Th concentration from the Lunar Prospector calibration for an area within the Feldspathic Highlands Terrane (0°–90°N and 120°–260°). For the Apollo sites we plot the Lunar Prospector Th concentration calculated [*Gillis et al.*, 2000] for pixels that include the Apollo 12, 14, and 16 landing sites against mean Th concentrations of typical soil samples from those sites [*Korotev*, 1998; *Korotev et al.*, 2000]. The areas containing the Apollo 12 and 14 landing sites are compositionally heterogeneous at the 2° scale. Thus we rebinned the Th data into 1° and 2° equal-area pixels that more accurately represent the geology of the landing sites and adjacent areas. The line is derived from a least squares linear regression weighted by uncertainties in both x and y values. The dashed line represents the 1:1 correlation that would be anticipated if the two calibration methods calculated similar Th abundances.

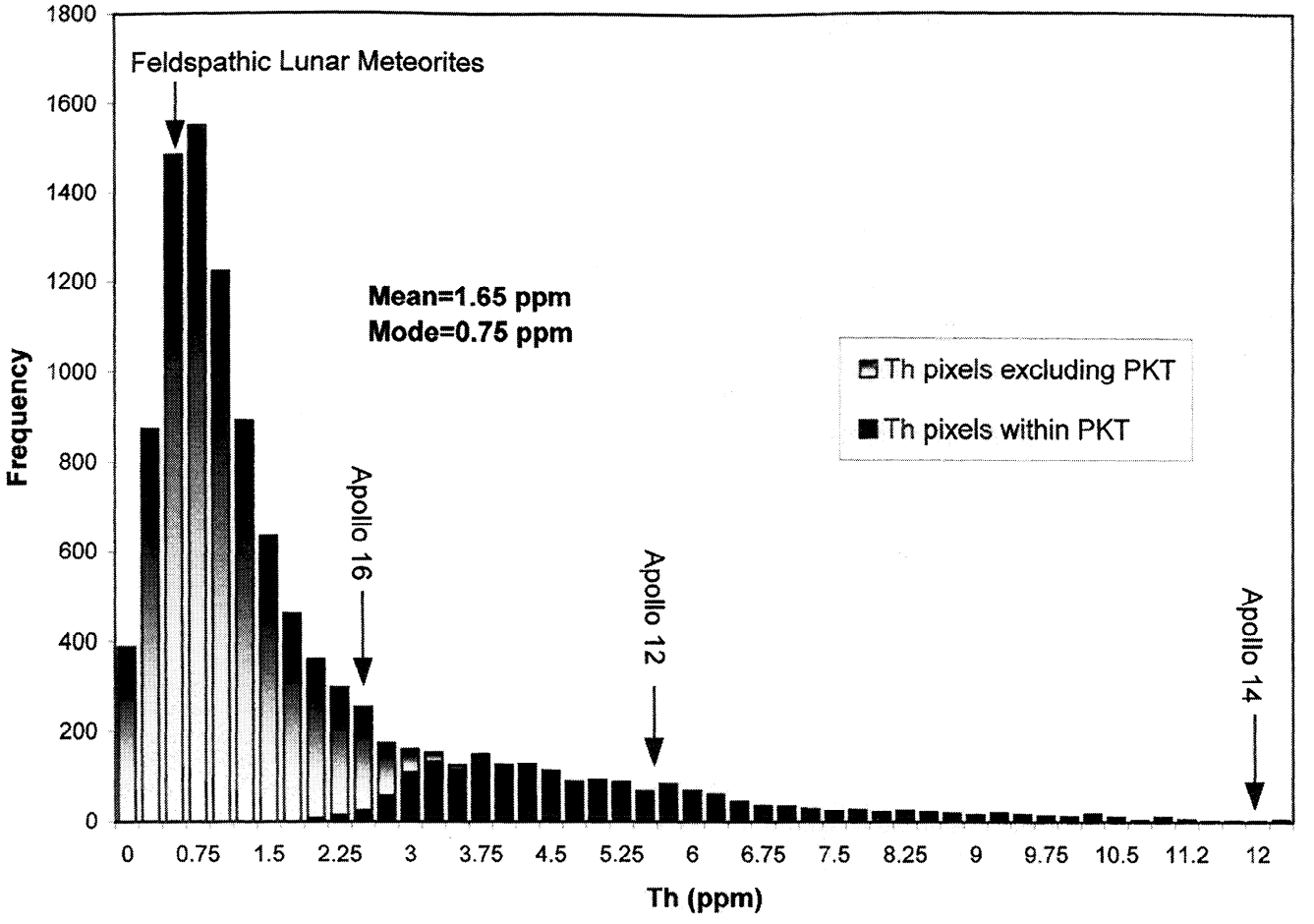

Figure 2. A histogram of global Th concentrations calculated using the regression from Figure 1. The distribution of Th concentrations for the Procellarum KREEP Terrane is shown in black. Most pixels with more than 3 Th ppm lie within the Procellarum KREEP Terrane, as do all pixels with more than 4.5 ppm Th.

most likely represent mixed regoliths.) This map is shown as Plate 2.

2.2. Lunar Prospector Thorium Data

Before discussing Th surface concentrations, we present our method and rationale for calibrating the Lunar Prospector γ-ray data. The low-altitude portion of the Lunar Prospector mission yielded a global map of thorium distribution at 2° resolution (equal area pixels, ~60 × 60 km at the equator) [*Lawrence et al.*, 1999]. For this map, absolute Th concentrations were derived on the basis of physical processes that are involved with creating and detecting γ rays in the spectral region of the main ^{232}Th γ ray (2.6 MeV). While comparing Th concentrations calculated by Lawrence et al. for pixels in which landing sites occur to Th concentrations for soils from those same sites, we observed a systematic discrepancy between the two sets of data. Because it is our purpose here to compare pixel compositions with samples, we needed an alternate, sample-based calibration. By fitting a linear relation between the Th abundances of Lawrence et al. and Th concentrations of regolith samples, we have constructed a ground-truth calibration (Figure 1). Both calibration methods are interim solutions until a rigorous determination of the detector efficiency and the 2.6 MeV γ-ray flux can be attained (e.g., spectral fitting and deconvolution analysis that takes into account contributions from higher-energy γ-ray lines and detector composition and geometry). These preliminary calibrations are possible because Th γ rays are produced by radioactive decay and hence do not depend on neutron flux. The intensity of the 2.6 MeV γ-ray line shows a considerable variation over the lunar surface, and it has few interfering lines from other elements. Because nearly all pixels within the Procellarum KREEP Terrane have >3 ppm Th, we expect that deviations from the assumed average background make only a minor contribution to fluctuations in Th concentration.

The ground-truth comparison is based on soil compositions at the Apollo 12, 14, and 16 landing sites as well as the mean compositions of the feldspathic lunar meteorites (Figure 1), which represent highlands regolith distant from the Apollo landing sites [*Palme et al.*, 1991; *Korotev*, 1999]. These four sampling sites were chosen because they are compositionally uniform at the 1° scale and span the range of Th concentrations observed on the lunar surface (Figure 2) [*Gillis et al.*, 2000]. For regions of low Th concentration (<2 ppm, Figure 1) the ground-truth calculation predicts lower Th concentrations than the calibration of *Lawrence et al.* [1999]. This difference is the result of the different procedures used by the two calibration techniques to calculate Th concentrations at low count rates. Our method depends on the average Th concentration of the feldspathic lunar meteorites (0.4 ±

0.2 ppm [*Korotev*, 1999]) and the γ-ray counts of the Feldspathic Highlands Terrane. In contrast, *Lawrence et al.* [1999] assume that the pixel with the minimum count rate has zero ppm Th. The offset of the regression line of Figure 1 (-0.75) shows that our calibration calculates negative Th concentrations at the lowest count rates. Although it is physically impossible to have negative Th concentrations, some negative measurement values are expected statistically when the uncertainty of the technique exceeds the measured value. Therefore a small number of negative Th abundances is acceptable and is expected. In addition to the discrepancy at low Th concentrations, we observe a 20% discrepancy between the ground-truth values and the theoretical calibration at high Th concentrations (Figure 1). This difference, although systematic, is close to the stated uncertainty of the theoretical calibration (~15% [*Lawrence et al.*, 1999]) and may be related to the response function of the gamma-ray spectrometer. Nevertheless, we choose to use our own calibration of the Lunar Prospector gamma-ray data in the subsequent discussion because our purpose is to compare Th concentration between pixels within the Procellarum KREEP Terrane and samples in the Apollo collection.

2.3. Clementine Data

The FeO and TiO_2 values were derived from the Clementine UVVIS data (415, 750, and 950 nm images), using an algorithm that is based on measured soil compositions for soils representing each of the sample stations from all of the Apollo landing sites [*Blewett et al.*, 1997; *Lucey et al.*, 1998, this issue]. For FeO, the calibration is driven by soil compositions from the Apollo 15 and Apollo 17 sample stations, especially the latter, which accounts for nearly half of the calibration points. For TiO_2, the calibration is heavily weighted by the Apollo 17 soils, which contain a high-Ti mare basalt component. Although we use the average FeO and TiO_2 calibrations to calculate surface compositions globally, we are aware that in some locations the average calibrations yield only approximate concentrations. For example, some of the measured Apollo and Luna soil compositions lie off the calibration curve for TiO_2, notably Luna 16, Luna 24, and Apollo 11; in these areas, TiO_2 concentrations appear to be significantly overpredicted by the average TiO_2 algorithm. In general, FeO values are more accurate than TiO_2 values; we note, however, that a calibration based on the low-Ti Apollo 15 basalts would yield higher FeO concentrations by 2 – 3 absolute percent FeO at the high end than the average FeO algorithm. Such a modified calibration may be appropriate for calculating the most accurate FeO concentrations from areas of low-Ti basalt.

3. Arguments Against the Presence of a Global Layer of KREEP-Rich Material

We define the boundary of the Procellarum KREEP Terrane as the edge of the contiguous region with surface Th concentrations of 3.0 ppm or greater (Plate 1). This boundary is somewhat arbitrary; for instance, *Jolliff et al.* [2000] defined the contour at 3.5 ppm Th or greater as the bounding edge. (The main reason for this difference is that we use the higher spatial resolution 2° data of *Lawrence et al.* [1999], whereas *Jolliff et al.* [2000] used the lower spatial resolution 5° data [*Lawrence et al.*, 1998].) The Procellarum KREEP Terrane is the only large lunar province that has such high surface Th concentrations. Of the 1926 pixels within our prescribed boundary, only 63 have Th concentrations <3 ppm, which emphasizes how pervasive the Th enrichment of this terrane is. The Procellarum KREEP Terrane is large, covering some 18% of the Moon's surface. Its boundary coincides approximately with the boundary of highly resurfaced Oceanus Procellarum and adjacent Mare Frigoris, it extends into Maria Humorum and Nubium and perhaps into western Mare Serenitatis, and all of Mare Imbrium lies within it. Most of the Procellarum KREEP Terrane has been resurfaced by basaltic volcanism. Outside of the resurfaced areas, cratered highlands rise 1 – 1.5 km above the maria, and Th concentrations taper off gradually into the surrounding Feldspathic Highlands Terrane.

The paucity of high surface relief breaching the smooth mare plains of the Procellarum KREEP Terrane is striking. We recognize that the Procellarum region was not produced by a single impact event [*Spudis*, 1993; *Neumann et al.*, 1996]. Even if there was a Procellarum impact basin (see *Whitaker* [1981] and *Wilhelms* [1987] for general discussions, and *Spudis* [1993] and *Neumann et al.* [1996] for dissenting evidence), more rugged terrain within the Procellarum KREEP Terrane would be expected than is observed. A succession of basin-sized impacts occurred within the Procellarum KREEP Terrane [*DeHon*, 1979; *Spudis*, 1993]; these would have renewed topographic roughness repeatedly. The only strong basin-related topographic features however, are those of the last basin-forming event within the terrane, Imbrium. Even Imbrium basin features (and, to a lesser extent, Serenitatis features) are suppressed compared with the systematics of basins outside the Procellarum KREEP Terrane [*Wieczorek and Phillips*, 1999]. Aside from the rings of Imbrium, the only other broad area of terra material to rise above the lava plains is the Fra Mauro Formation near the Apollo 14 site, which lies on an area of elevated topography that may be the remnants of ancient basin ejecta or intersections of basin structures (e.g., the Cognitum, Insularum, Nubium, and Stadius-Aestuum basins).

Production of large craters surely occurred within the Procellarum KREEP Terrane just as we see in the surrounding Feldspathic Highlands Terrane, but the rugged topography expected from such large crater production is nearly absent. Large, ancient craters near the edge of Oceanus Procellarum are visible, but they show greater relaxation than their counterparts in the nearby Feldspathic Highlands Terrane. We recognize that lavas have filled and smoothed the preexisting topography to some extent. These lavas are typically ~500 m thick, however, as shown by *DeHon* [1979] on the basis of mare filled and embayed craters. Therefore, had the terrane not relaxed, the rims of simple craters larger than a few kilometers might be expected to poke up through the maria, assuming a depth/diameter of ~1/5 [*Croft*, 1980], but few do.

The expanse of subdued relief within the Procellarum KREEP Terrane, and to some extent the Serenitatis basin [*Wieczorek and Phillips*, 1999, this issue], argues for an internal heat source that kept the terrane hot through the period of heavy meteoroid bombardment, enabling crustal relaxation that diminished crater elevation and gave rise to subsequent, extensive volcanism. In comparison, the Moon's largest basin, South Pole-Aitken, retains considerable relief from basin-sized impacts that occurred after it formed but prior to the formation of Mare Imbrium. It apparently underwent no relaxation comparable to that of the Procellarum KREEP Terrane. A plausible heat source for crustal relaxation as well as extensive volcanism is high concentrations of Th and other radioactive elements extending from near the surface to depth. The absence of areally extensive crustal relaxation and extensive mare volcanism in other parts of the Moon indicates that the distribution of KREEP is not uniform; there is no global layer rich in incompatible trace elements. These elements were

somehow concentrated in a small region of the Moon and gave rise to the Procellarum KREEP Terrane.

Maria occur outside the Procellarum KREEP Terrane, and their presence is indirect evidence for additional subsurface reservoirs of heat. This heat might also be a consequence of high concentrations of radioactive elements at depth. The ejecta of the basins containing these maria and most of the mare basalts themselves have low Th concentrations, although those concentrations are perhaps modestly higher than those of the surrounding feldspathic materials [*Jolliff et al.*, 2000].

4. Terrae (Nonmare) and Mixed Regions of the Procellarum KREEP Terrane

4.1. Terrae Definition and Distribution

"Terra" in this paper is synonymous with "nonmare." Locations of the terra pixels are shown in Plate 2. Because there is no evident, systematic compositional difference between the more rugged and the more gentle nonmare regions (e.g., Imbrium rim formation and Fra Mauro formation), we make no distinction among different types of terrae. Terra regions are not randomly distributed; those with lower Th and lower FeO concentrations occur mainly toward the periphery of the terrane. Especially within the terrane, only a fraction of the areas of terra are broad enough to fill at least 90% of a 2° pixel (typical distance ~60 km). Mainly for this reason, pixels classified as terrae with Th concentrations >6 ppm are sparse; most of them occur in the following locations: highland areas surrounding Mare Vaporum, north to the Apennines, where they intersect the Haemus Mountains, and south into the Central Highlands and from there to the east; in the Fra Mauro region; in the highlands northwest of Mare Humorum and the crater Gassendi; south and west of Sinus Iridum, especially near the crater Mairan; northeast of Sinus Iridum; western Oceanus Procellarum near the crater Lavoisier; and discontinuously along the north and south sides of Mare Frigoris from about 30° west to 30° east longitude.

Most pixels with high Th concentrations (>6 ppm) are classified as "mixed." These pixels contain much of the terrae well within the boundary of the Procellarum KREEP Terrane. Most of them are found in the following locations: a broad area that extends from Kepler to the Carpathians and from west and south of Copernicus through the area of crater Reinhold to the northern extents of Mare Nubium and eastward to the western central highlands at ~5°W; the region from Timocharus east across the Apennine Bench into the Apennines, north to Aristillus and east into the Caucasus; the region surrounding Aristarchus; and the highland region around Sinus Iridum, then along the northern rim of Mare Imbrium, and along the edges of Mare Frigoris.

4.2. Terrae as Basin Rim and Ejecta

Terrae within the interior of the Procellarum KREEP Terrane occur mainly as Imbrium basin rim or ejecta deposits. Their igneous character and original stratigraphy were probably destroyed by the impact process that produced that basin. The average thickness of Imbrium ejecta deposited on the Procellarum KREEP Terrane, on the basis of the equations of *Housen et al.* [1983] and a transient crater radius of 370 km [*Wieczorek and Phillips*, 1999], ranges from ~2800 m at 2 transient crater radii from the center of Imbrium (~740 km, roughly the distance to Copernicus) to ~1000 m at the distance of 3 transient crater radii (1160 km, nearly the distance to Fra Mauro) to ~600 m at 4 transient crater radii (1530 km, about the distance to the center of Mare Nubium). Although the deposits from these ejecta may erase or degrade preexisting craters, they do not account for the generally low elevation of the terrane. The above values are estimates of average thicknesses of the ejecta themselves; the average ejecta deposits would be significantly thicker (by ~2.5 times at the distance of 3 transient crater radii) according to the ballistic sedimentation model of *Oberbeck* [1975; *L. A. Haskin et al.*, unpublished results, 2000] because the ejecta would have excavated the substrate onto which they impacted and would have mixed with it. (*Schultz and Gault* [1975] have argued that little excavation and mixing would have occurred, however).

The Th-rich Imbrium ejecta presumably represent materials from a thick section (tens of kilometers) of the pre-Imbrium crust of the Procellarum KREEP Terrane that was excavated by the Imbrium event. The Th enrichment of the Procellarum KREEP Terrane evidently extends to a considerable depth. As a consequence of this high concentration of Th and other radioactive elements, the crust of the Procellarum KREEP Terrane may have remained hot throughout the period of heavy bombardment prior to ~3.9 Ga [e.g., *Longhi*, 1989; *Ryder*, 1994; *Haskin*, 1998; *Wieczorek and Phillips*, this issue]. This would account for the high proportion of melt in Imbrium ejecta if the ejecta are indeed mainly represented by the impact-melt breccias as suggested by *Haskin et al.* [1998].

If Th-rich Imbrium ejecta were mixed with Th-poor terra from the rest of the Procellarum KREEP Terrane, there would be a decrease in Th concentration as a function of distance away from the Imbrium basin for terra and mixed pixels within the terrane, as is observed outside of the Procellarum KREEP Terrane and throughout the Feldspathic Highlands Terrane [*Haskin*, 1998]. No trend of decreasing Th concentration away from the Imbrium basin is evident within the terrane (Plate 1), however, indicating that the substrate with which Imbrium ejecta mixed was also Th rich, a conclusion that adds to the evidence of subdued morphology and extensive volcanic resurfacing for a terrane-wide enrichment in Th. Furthermore, the alkali and magnesian-suite plutonic rocks, which are differentiates of Th-rich magmas and which predate the Imbrium impact, appear to be of relatively shallow crustal origin [e.g., *McCallum and O'Brien*, 1996; *Jolliff et al.*, 1999], indicating that high-Th material was at or near the surface before the Imbrium event occurred. The overall high Th concentration of the terrane is thus not simply a consequence of the excavation of the Imbrium basin even though part of the terrane is covered with material excavated from that basin.

4.3. Terra Chemistry

In a plot of FeO versus Th (Plate 3a), the data for all the pixels within the Procellarum KREEP Terrane define a roughly triangular pattern, a "data polygon." This data polygon lies within a triangle whose apices correspond to well-known materials in the lunar sample collection, as described below. In the plot of FeO versus Th (Plate 3a), the terra pixels lie along the low-Fe edge of the data polygon. They range in Th concentration from 2 to 12 ppm and in FeO concentration from 4 to ~11%. On the plot of TiO_2 versus FeO (Plate 4a), the terra pixels with <11% FeO have an average of 0.7% TiO_2, but they range as high as 2%. For the terra pixels taken as a group, concentrations of FeO (as in Plate 3a) and TiO_2 are moderately correlated ($r = 0.74$), and those of Th and FeO are slightly less well correlated ($r = 0.65$). Those of Th and TiO_2 are not significantly correlated, possibly because low TiO_2 values are known only to low precision [*Lucey et al.*, 1998]. For more specific locations, correlations or anticorrela-

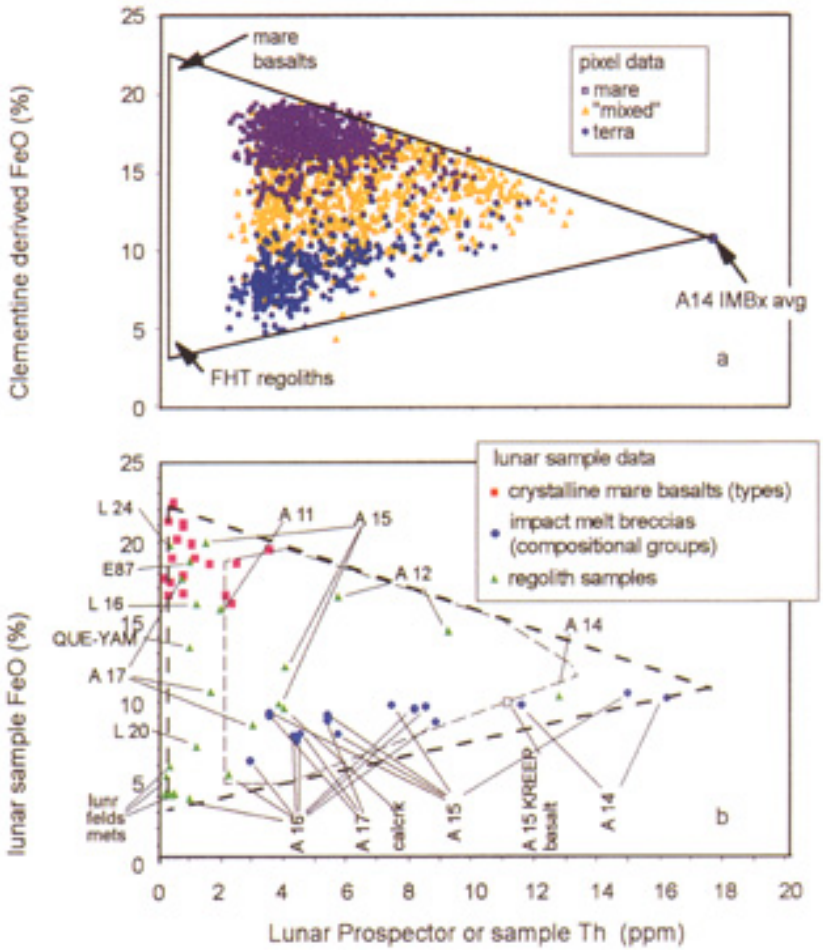

Plate 3. (a) Clementine-derived FeO concentrations are plotted against Lunar Prospector Th concentrations for the three pixel types, mare (open squares), terra (open diamonds), and mixed (triangles), of the Procellarum KREEP Terrane. The pixel data lie within a triangle bounded by mare basalt, typical regolith of the Feldspathic Highlands Terrane, and Apollo 14 high-Th impact-melt breccias. As explained in the text, the FeO values for many of the mare pixels may be ~2 absolute percent FeO too low, so the separation between terra and mare pixels may be greater than shown. (b) Sample averages are shown for mare basalts, regolith samples, and impact-melt breccias. The polygon that circumscribes the pixel data of Plate 3a is included for comparison.

tions occur, as shown below. Some of the terra pixels reach the low FeO and TiO_2 concentrations of feldspathic material typical of the Feldspathic Highlands Terrane (4.5% and <0.5%), but none reach the low Th concentrations (<0.5 ppm) found in the feldspathic lunar meteorites presumed to come from that terrane. Pixel-sized regions of highly feldspathic terra (≤5% FeO) within the Procellarum KREEP Terrane are rare.

Three Apollo sites (12, 14, and 15) lie within the Procellarum KREEP Terrane, so some materials originating within that terrane have been sampled. Impact-melt breccias representing Imbrium ejecta are also found at sampling sites outside the terrane. It is thus not surprising that in the lunar sample collections, several types of materials have compositions that fall within the same range as the terra pixels of the Procellarum KREEP Terrane. Among these, the impact-melt breccias are the most abundant materials whose compositions cover about the same range as the terra pixels. These breccias, overall, can be modeled as variable mixtures of material of intermediate Mg/Fe KREEP-norite composition, feldspathic materials, and high Mg/Fe olivine (<20%) [*Korotev,* 2000]. The composition of the KREEP-norite ranges from 6 to 20 ppm Th and from 10 to 11% FeO [*Korotev,* 2000]. Much like regolith samples taken from the Procellarum KREEP Terrane, the regoliths of the terra pixels correspond in composition to mixtures mainly of KREEPy noritic material and feldspathic material. For comparison, regolith collected from the Apollo 14 site occurs at the high-Th end of the range of terra pixels (i.e., ~10% FeO and 13 ppm Th [*Jolliff et al.,* 1991]) and is dominated by KREEP-norite-rich melt breccia. Regolith from the Apennine Front at Apollo 15 (i.e., 10% FeO and 3.8 ppm Th, from the bottom of the station 2 core, where it is least contaminated with mare material [*Korotev,* 1987]) has a composition near the low-Th end, where the main cluster of terra pixels occurs, and contains a higher proportion of low-Th feldspathic material and a lower proportion of the KREEPy melt breccia. If we presume that the impact-melt breccias are the principal ejecta from the Imbrium basin, then the average composition of the predominant material of the pre-Imbrium Procellarum KREEP Terrane to the depth of sampling of the Imbrium basin was that of the KREEP-

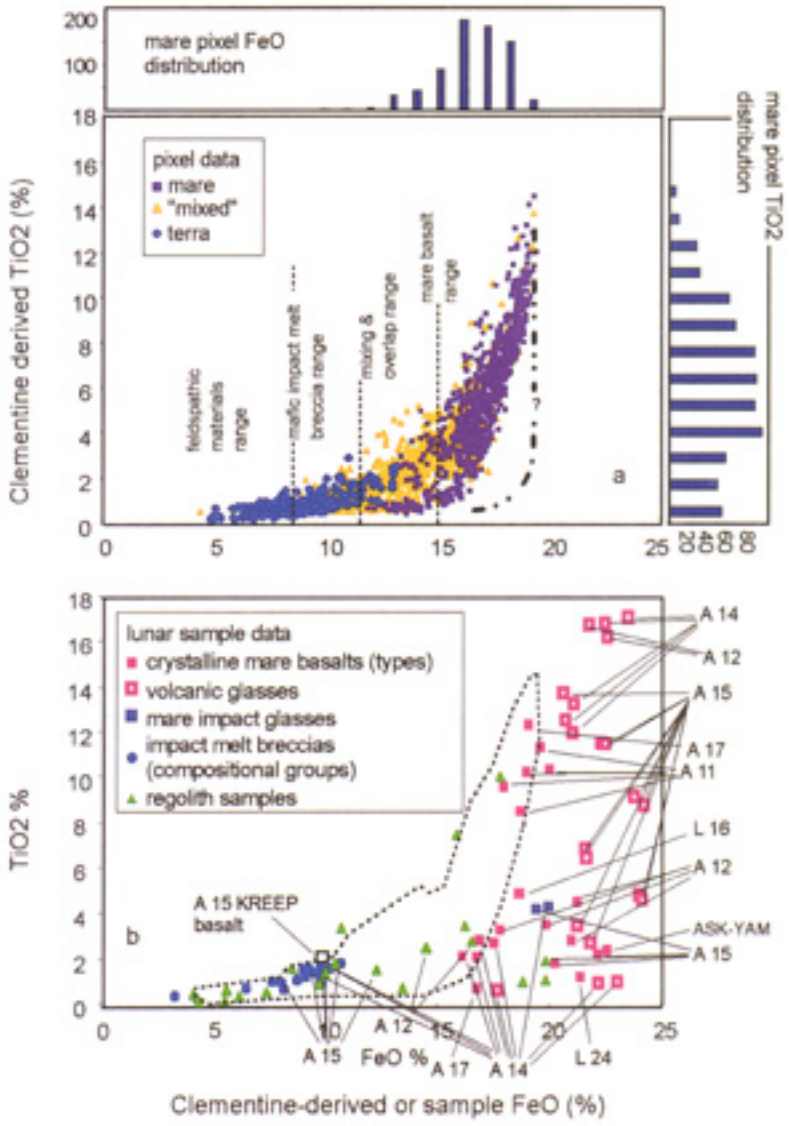

Plate 4. (a) Clementine-derived FeO concentrations are plotted against Clementine-derived TiO_2 for the pixels of the Procellarum KREEP Terrane. For mare pixels there is a steep rise in slope beginning at ~16% FeO and ~2% TiO_2. This slope appears to be a consequence of the manner in which the parameters were obtained for the algorithm that converts the Clementine spectral data for low- and intermediate-TiO_2 mare regoliths to FeO concentrations, rather than an actual FeO-TiO_2 correlation. Histograms show that FeO values peak at ~16% for the mare regoliths, a value that seems low, so we suggest that the data for these pixels should be shifted to higher values of FeO to a more nearly vertical relationship, as shown by the dashed line. Histograms for TiO_2 indicate that most of the basalts of the Procellarum KREEP Terrane have higher TiO_2 concentrations than the basalts sampled at the Apollo 12 and 15 sites. (b) Average values of FeO and TiO_2 are plotted for materials from the sample collections. Except for the Apollo 14 samples, the mare basalts and the volcanic glasses plot more nearly vertically, as suggested for the data in Plate 4a. An outline of the data in Plate 4a is shown in Plate 4b. Note also that no pixels correspond to mixed subequal areas of high- or intermediate-TiO_2 mare regolith and terra-dominated regolith. This occurs because the main areas of intermediate- and high-TiO_2 Procellarum-Imbrium maria have relatively few occurrences of terra, so mare-terra boundaries are uncommon.

norite component. The olivine and feldspathic components of the breccias were subordinate materials of the terrane. KREEP-rich material is found in the sample collections only as KREEP basalt and as a component of impact breccias and glasses; it has not been observed in the samples as a plutonic rock type. The feldspathic material in the lower-FeO terra pixels may be similar to that of the Feldspathic Highlands Terrane and may in fact come from that terrane, as most of those terra pixels lie near the boundary between the Procellarum KREEP Terrane and the Feldspathic Highlands Terrane. Regolith samples obtained from the Procellarum KREEP Terrane also span a range of compositions and consist mainly of feldspathic and KREEPy materials.

5. Mare Regions of the Procellarum KREEP Terrane

5.1. Mare Lava Plains

The resurfaced volcanic plains are the most prominent morphologic feature of the Procellarum KREEP Terrane (Plate 2). Broad, continuous expanses of mare pixels are observed, with some 38% of the pixels qualifying as mare (i.e., containing >90% mare plains). Many more pixels (44%) partly containing mare plains are designated as "mixed." Lavas of Imbrian and Eratosthenian age cover most of Oceanus Procellarum and Maria Imbrium, Cognitum, Frigoris, Humorum, Nubium, Vaporum, and western Serenitatis (Plate 2). These plains postdate the heaviest meteoroid bombardment, and large areas of them occur at a substantial distance from major mare-terra boundaries, so lateral contamination from distant regions of terra should be minimal. The mare plains are disrupted in some locations where craters have penetrated into terra beneath them, but obvious occurrences of this type are relatively rare (e.g., Kepler, Aristarchus, Aristillus Copernicus, Reinhold, Timocharis, Pytheas). Pixels dominated by mare basalt and having FeO concentrations higher than 18% occur in western and southwestern Oceanus Procellarum and in some parts of Mare Imbrium. Mare pixels with the lowest apparent FeO concentrations (≤14%) are located along the boundary of Mare Frigoris, along the southeastern rim of Mare Imbrium near Fra Mauro, and within Mare Imbrium near the crater Aristillus.

The mare regions that have the highest TiO_2 concentrations (Plate 2) are mainly Eratosthenian in age [*Wilhelms and McCauley,* 1971]. These regions are nearly free of exposures of terra that rise above the mare plains. They are also nearly free of late craters that might have penetrated into the terrae beneath; craters such as Euler, Reiner, and Schiaparelli appear to have exhumed only older mare, not terra. Modes of contamination with terra are thus few, so we may expect mixing of terra material into the regolith of these Eratosthenian plains to be relatively minimal. This is consistent with the restricted mixing of terra into high-Ti mare pixels described above (Plate 4a). (Given the long reach of crater rays, this does not mean that we should expect the regoliths covering the youngest mare regions to be entirely free of terra material, however.)

Some mare areas (e.g., Marius Hills, Aristarchus Plateau, Mare Vaporum, Sinus Aestuum [e.g., *Gaddis et al.,* 1985; *Hawke et al.,* 1989]) have dark mantling deposits. Where these are prominent, we have classified the pixels as "mixed." Such deposits do not cover a high fraction of the mare plains.

5.2. Is There an FeO-TiO_2 Trend?

The distribution of TiO_2 concentrations in the mare pixels of the Procellarum KREEP Terrane is continuous from <1% to ~15% TiO_2. *Giguere et al.* [2000] found a continuous distribution of mare TiO_2 concentrations moonwide, and much of the mare basalt-dominated area of the Moon lies within the Procellarum KREEP Terrane. Giguere et al. report that only some 20% of the maria have more than 5% TiO_2. In the Procellarum KREEP Terrane, over 50% of the mare pixels have more than 5% TiO_2. In the plot of Clementine-derived FeO versus TiO_2 data (Plate 4a), we note that the distribution of the data (mare pixels, mainly) along the high-FeO side slopes from moderate FeO (~16 wt%) at low TiO_2 concentration to high FeO (~19 wt%) at high TiO_2 concentration. This trend is difficult to explain in terms of mixing of known rock compositions. The lack of pixels extending to high FeO at low TiO_2 is especially puzzling given the FeO-rich compositions of many low-Ti Apollo basalts. This trend, if sustained, would imply that the mare pixels that represent lower-Fe, lower-Ti basalt regions are, without exception, mixed systematically and extensively with lower-Fe terra materials, whereas pixels representing regions of higher-Ti basalts are not mixed with appreciable terra. If this trend were correct, it would be a surprising and important result; no such trend is observed among analyzed samples of mare basalts or volcanic glasses (Plate 4b). (On the basis of the mass balance alone, a trend of decreasing TiO_2 with decreasing FeO concentration can be produced mathematically by simple addition of ilmenite to a low-Ti mare basalt. For example, addition of 20% ilmenite to Apollo 12 pigeonite basalt increases the FeO concentration from 20 to 25% and the TiO_2 concentration from 1.8 to 10%. There is no evidence that mare basalts are actually produced by such massive assimilation of TiO_2, however.)

Although physical mixing related to impact processes remains a possibility, we are suspicious that the trend results from our use of the average algorithm to calculate FeO from the global Clementine data (discussed above). The Apollo 15 soils, whose FeO concentrations are dominated by low-Ti mare basalts, define a slightly different calibration when considered by themselves. This calibration, if applied to similar high-Fe, low-Ti regions, would likely produce FeO concentrations as much as ~2 – 3 absolute percent higher than shown in Plate 4a. Such a modification would shift the lower right corner of the FeO-TiO_2 distribution to higher FeO concentrations, producing a nearly vertical array for those pixels dominated by mare basalt, as indicated by the dashed line in Plate 4a. This recalibration would also shift the FeO values for most of the mare pixels and some mixed pixels upward toward the highest concentrations shown in Plate 3a.

5.3. Mare Chemistry

The mare pixels determine the high-FeO side of the data polygon, and mare basalts account for the high-FeO apex of the triangle in Plate 3a. Most of the mare regoliths have Th concentrations between 2.5 and 7 ppm, and some have even higher concentrations. These concentrations are much higher than those of the mare basalts from the Procellarum KREEP Terrane sampled by the Apollo missions (some aluminous basalts of Apollo 14 have as much as 4 ppm Th, but whether these represent extensive flows within the Procellarum KREEP Terrane is not actually known). Mare pixels have FeO concentrations that range from 10 to 19.5% FeO (using the global FeO algorithm as described in section 2). The average for sampled mare basalts is at the high end of this range, 20% FeO, and averages of individual types of sampled mare basalts range between about 17 and 22%. The FeO concentrations of the mare pixels (mostly >15%) indicate that at the pixel scale the lavas are mare basalt and not KREEP basalt

(10% FeO). The mare regoliths also show a substantial range of TiO_2 concentrations, from 0.5 to 14.5%. High TiO_2 concentrations are known among some Apollo 11 and 17 mare basalts (up to nearly 13%). High TiO_2 concentrations are not found among Apollo 12, 14, and 15 mare basalts, however, and those basalts were collected from the Procellarum KREEP Terrane. *Pieters* [1978] and *Pieters et al.* [1980], on the basis of ground-based VIS-NIR spectral data, have indicated that broad expanses of unsampled types of mare basalts are present within the Procellarum KREEP Terrane, and *Giguere et al.* [2000] found a continuum of TiO_2 concentrations based on Galileo and Clementine data. The mare surfaces of the Procellarum KREEP Terrane have a prevalence of concentrations in the range of 4 – 8% TiO_2 (Plate 4a). Among the mare pixels of the Procellarum KREEP Terrane taken as a group, Th concentrations are not correlated with FeO or TiO_2 concentrations (not shown). We next consider whether the mare pixels represent regoliths in which the high Th concentrations are in the basalts themselves, or whether they represent regolith composed mainly of low-Th basalts mixed with high-Th terra.

5.4. Arguments Favoring Low Th Concentrations for the Mare Basalts of the Procellarum KREEP Terrane

The materials from the Procellarum KREEP Terrane in the sample collections that have exceptionally high Th concentrations (e.g., >10 ppm) are nonmare. Arguments have been made for KREEP assimilation to account for the raised Th concentrations of the Apollo 11 high-K and the Apollo 14 aluminous basalts [*Dickinson et al.*, 1985; *Shervais et al.*, 1985a, b; *Shih et al.*, 1986; *Shearer and Papike*, 1993; *Hess and Parmentier*, 1995]. Strictly on the basis of observed Th concentrations in the main samples of mare basalt obtained within the Procellarum KREEP Terrane, however, there would be little reason to expect high Th concentrations in the mare basalts.

High-Th terra is exposed in many locations within the Procellarum KREEP Terrane, and where it is not exposed at the surface, it probably underlies the mare plains. Vertical mixing is evident around some relatively fresh craters, and such mixing may be ubiquitous. This mixing may not be obvious in the geomorphology, however, if small enough cratering events caused it. Accessible nonmare materials could be present in more than one form. Although *Ryder* [1994] has suggested that KREEP basalt volcanism was triggered by the Imbrium impact, volcanism of this general type may not have been restricted to just one location and a short period of time. If some form of KREEP basaltic volcanism occurred more widely than is evident, KREEP basalt flows may lie stratigraphically between mare basalt flows. If so, they could be near the surface and accessible by shallow impact cratering, but their presence would not be geomorphologically evident. Similarly, impacts through earlier mare basalt flows into the terra substrate may have occurred, but the ejecta may have been covered by later basalt flows so they are no longer evident. These ejecta deposits, too, might be accessible by shallow cratering. Vertical mixing in these circumstances could contribute high-Th terra materials to the mare pixel regoliths.

It is possible to select a Th-rich terra material known from the sample collection that can be mixed with mare basalt of reasonable FeO and TiO_2 concentrations to account for the FeO, TiO_2, and Th concentrations of any mare pixel. A single mare basalt composition, however, cannot account for all such mixtures; a range of TiO_2 concentrations in the mare basalts is required, but that is reasonable. Similarly, a single terra component, particularly one with a narrow range of Th concentrations, cannot account for these compositions, but a range of Th concentrations in the terra is known to occur. Terra materials with major-element compositions that can be used to satisfy mixing constraints include Apollo 15 KREEP basalt and Apollo 14 mafic impact-melt breccia. If the FeO concentrations of the low-Ti mare pixels are correct as shown in Plate 4a, the required amount of mixing with terra material is implausible (≥50% terra in some cases). If the Clementine-derived FeO concentrations for the low-Ti mare pixels are too low by a few absolute percent (section 5.2), a terra source for the high Th concentrations of the mare pixels cannot be ruled out on the basis of known chemical constraints.

5.5. Arguments Favoring High Th Concentrations Indigenous to Mare Basalts of the Procellarum KREEP Terrane

As pointed out above, mare pixels cover broad expanses of the Procellarum KREEP Terrane, and many of these pixels are remote from obvious, exposed sources of high-Th terra materials that might supply Th to the regoliths. This is especially true for the flows of Eratosthenian age. There is no obvious geomorphologic evidence for extensive mixing with terra. (The regolith at the Apollo 12 site is nevertheless an example of extensive mixing of high-Th terra of unknown provenance with mare basalt [*Korotev et al.*, 2000; *Jolliff et al.*, 2000], and even allowing for a Copernicus ray, reasons for such extensive mixing are not clear.) The highest concentrations of FeO in the mare pixels reach 19.5%, about average for sampled mare basalts, lower than some sampled mare basalts (up to 23%) but much higher than the sampled mare-dominated regoliths (11.5 – 15.5%) [*Korotev*, 1998]. This high FeO concentration leaves little room for significant contamination of mare regolith by terra materials that could supply the Th, except for the most Th-rich terra materials such as quartz monzodiorite or lunar granite (35 – 40 ppm). Those terra materials are rare among the high-Th materials of the sample collection, however, and the possibility that they are present in high abundance in the Procellarum KREEP Terrane is not supported by similarly high Th concentrations of terra pixels.

As previously indicated, there are no terrane-wide correlations between Th and FeO or TiO_2 for the maria. Traverse profiles across different geomorphologic units show interpretable systematics, however. Data for all three elements are shown in Figure 3 for a profile of pixels at 47° west longitude. Note the long distance (8°S - 20°N, 850 km) over which FeO is constant and >18%, indicating mare regolith with little intermixed terra material. Concentrations of TiO_2 are intermediate and variable, ranging between 7 and nearly 12%. Concentrations of Th are also somewhat variable at ~5 ± 1 ppm. The pattern of the FeO points is only roughly matched by the TiO_2 concentrations, most strongly where a transition between mare and mixed pixels occurs. The gradient in Th concentration away from Aristarchus extends ~6° on each side of the Th peak, a total distance of 360 km. The 5 ppm Th is most likely the concentration of the basalts themselves. Other profiles tested also lead to the conclusion that some mare basalts are Th-rich compared with most sampled basalts.

There is also some support from sample data for this conclusion. Although large specimens of high-Th, high-Ti mare basalt are not included among the samples collected from the Procellarum KREEP Terrane, two materials that bear on the possibility of such basalts are present. The volcanic glasses of mare affinity (the "picritic" glasses of *Shearer and Papike* [1993] and *Papike et al.* [1998]; Plate 4b) show a range of TiO_2 concentrations similar to that of the mare pixels. There are no data for Th concentrations of these glasses, but there are data for REE concen-

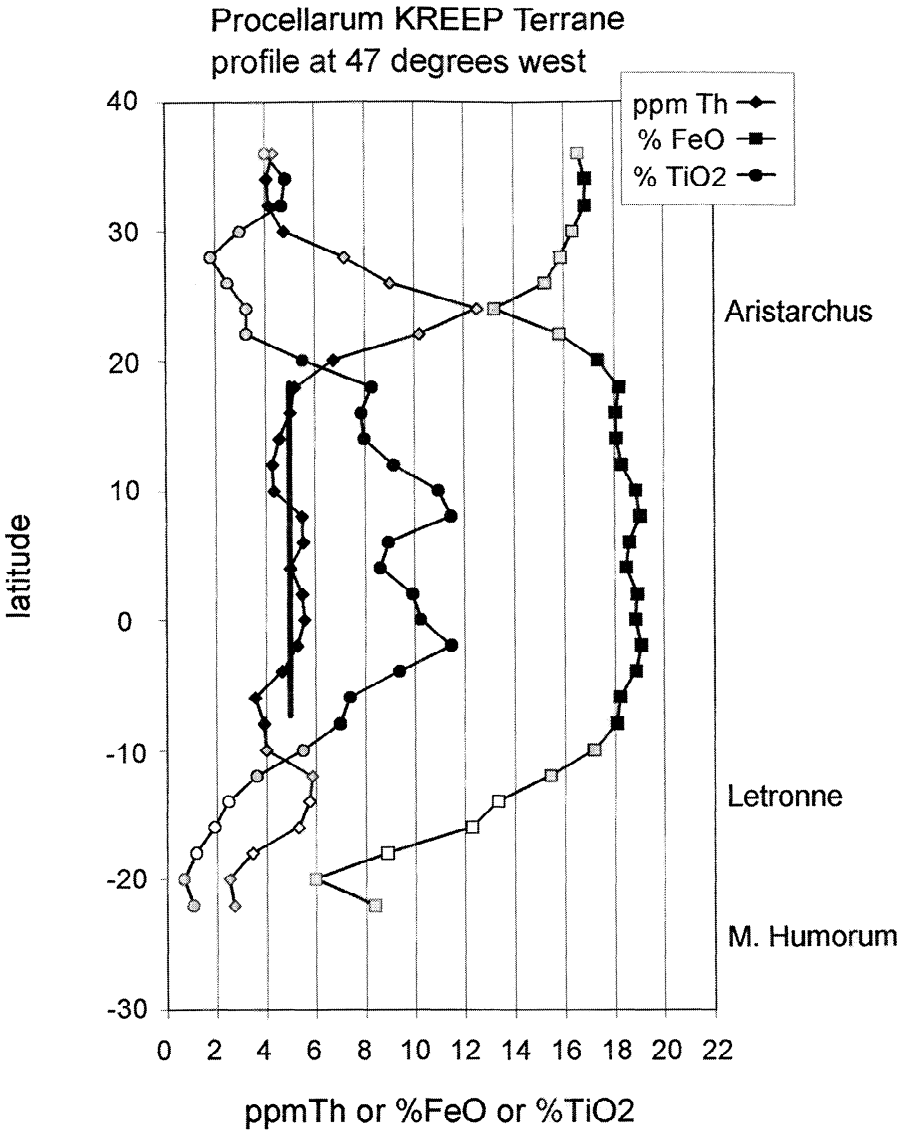

Figure 3. A traverse profile of Th, FeO, and TiO_2 concentrations for pixels centered along 47° W longitude. Mare pixels are black, "mixed" pixels are gray, and terra pixels are unfilled. The profile begins in northern Mare Humorum, passes through terra and mixed terrain into Oceanus Procellarum, crosses eastern Aristarchus, and continues north into Oceanus Procellarum again. Latitudes for Aristarchus and Letronne, near which the profile passes, are indicated. The range of evident mixing of high-Th Aristarchus material and basalt extends from latitudes ~18° to 30° N latitude, a distance of some 360 km. The bar through the Th data between 8° S and 20° N latitude emphasizes the high Th concentrations over some 850 km of uninterrupted high FeO concentrations. Note that concentrations of TiO_2 vary considerably (from 4 to 7% TiO_2) in the mare-dominated regions. Concentrations of FeO vary sympathetically with those of TiO_2 (17 to 19% FeO). This may reflect the calibration of the Clementine data for FeO rather than an actual variation (see caption to Plate 4 and text). The dips in FeO concentration are not accompanied by an increase in Th concentration, as would be expected if the FeO were diluted by high-Th terra and as is observed near Aristarchus.

trations. Some of the REE distributions tend toward a KREEP-like pattern. If we use the Th/Sm ratios of KREEPy materials, we can estimate Th concentrations for the glasses. These estimates range from 2 to 5 ppm, roughly the same range as observed for the mare pixels. The Th/Sm ratios in sampled mare basalts are lower than that of KREEP, however, and their use would not yield such high Th concentrations. Two samples of impact glass from the Procellarum KREEP Terrane that have major element compositions of mare basalt have been studied. One is an Apollo 15 yellow impact glass clod with 8 ppm Th, 19% FeO, and 4.2% TiO_2 [*Delano et al.*, 1982], and the other is an Apollo 14 glass bead with 5.4 ppm Th, 20% FeO, and 4.4% TiO_2 [*Jolliff et al.*, 1991]. These volcanic and impact glasses offer some support that high-Th, high-Ti basalts exist within the Procellarum KREEP Terrane. Concentrations of 2 - 7 ppm Th in some mare basalts of the Procellarum KREEP Terrane thus appear reasonable.

6. Summary of Characteristics of the Procellarum KREEP Terrane and Speculations on Its Origin

The global data sets from the Clementine and Lunar Prospector missions in combination with the geomorphology have enabled us to extend observations of lunar sample chemistry to the Procellarum KREEP Terrane overall. The combined information is consistent with terrane-wide enrichment in Th and other trace elements to a substantial depth (tens of kilometers). Owing to its high concentrations of the heat-producing trace elements K, U, and Th, the terrane remained hot longer than other parts of the Moon's crust, and we suggest that the high temperature in combination with the large size of the Imbrium basin-forming event caused a large proportion of the material excavated from that basin to be ejected as melt. This melt is observed in the sample collection in the form of impact-melt breccias, and these may be the principal form of Imbrium ejecta. If so, the crust of the Procellarum KREEP Terrane is more mafic than that of the Feldspathic Highlands Terrane as well as more trace-element-rich. The materials of the Imbrium basin rim and of the Fra Mauro Formation represent mixed sections of the pre-Imbrium crust of the Procellarum KREEP Terrane, and these materials are Th-rich. So pervasive is the high trace-element content of the Procellarum KREEP Terrane that some of the mare basalts of the terrane appear to have Th concentrations much higher than is typical of the sampled mare basalts. Because the Procellarum KREEP Terrane is unique as a large, trace-element-rich province, basin-sized impacts into its crust would have spread Th-rich ejecta across the terrane and beyond, and are the main form of Th in the adjacent Feldspathic Highlands Terrane.

We speculate on the origin of the Procellarum KREEP Terrane as follows: The mechanism for its formation probably requires that late-stage, Fe-rich residual melt (urKREEP?) from a very large amount of magma (possibly a global magma ocean) accumulated there to a degree not matched elsewhere on the Moon. The high concentrations of heat-producing elements in this terrane maintained a high temperature that is reflected in the subdued topographic relief of the terrane and the high proportion of melt in Imbrium ejecta. The terra (nonmare) materials of the terrane are more feldspathic toward the periphery where mixing presumably occurred with crustal materials of the Feldspathic Highlands Terrane. In the interior, where they occur as Imbrium rim and ejecta deposits, they are richer in KREEP-bearing material of noritic composition. The intermediate Mg/Fe of this noritic material implies that the Fe-rich residual melt reacted with more magnesian materials [e.g., *Warren,* 1988]. This contact with more magnesian materials probably came about through sinking because of the high density of the Fe- and Ti-rich residual melt and its crystallization products, as suggested by others [e.g., *Herbert,* 1980; *Hess and Parmentier,* 1995]. On contact with materials of higher Mg/Fe, reaction and melting produced materials of lower density that rose to produce the relatively mafic crust of the terrane [e.g., *Wieczorek and Phillips*, in this issue]. Heat from the deep column of KREEP-rich material led to extensive mare volcanism, and, like other petrogenetic products of the terrane, the mare basalts have relatively high Th concentrations.

Acknowledgments. We thank the Lunar Prospector Team for making available the Th data (http://nis-www.lanl.gov/nis-projects/lunar). We thank D. Lawrence for re-binning the Lunar Prospector Th data for the Apollo 12 and 14 landing sites. We thank Mark Wieczorek for informative discussions. We appreciate reviews of the initial manuscript from P. Schultz and an anonymous reviewer. This work was funded in part by the National Aeronautics and Space Administration under grants NAG5-4172 (LAH), NAG5-6784 (BLJ), and NAG5-8609 (RLK).

References

Binder, A. B., Lunar Prospector overview, *Science*, *281*, 1475–1476, 1998.

Blewett, D. T., P. G. Lucey, B. R. Hawke, and B. L. Jolliff, Clementine images of the lunar sample-return stations: Refinement of FeO and TiO_2 mapping techniques, *J. Geophys. Res.*, *102*, 16,319–16,325, 1997.

Croft, S. K., Cratering flow fields: Implications for the excavation and transient expansion stages of crater formation, *Proc. Lunar Planet. Sci. Conf. 11th*, 2347–2378, 1980.

DeHon, R. A., Thickness of the western mare basalts, *Proc. Lunar Planet. Sci. Conf. 10th*, 2935–2955, 1979.

Delano J. W., D. H. Lindsley, M.-S. Ma, and R. A. Schmitt, The Apollo 15 yellow impact glasses: Chemistry, petrology, and exotic origin, *Proc. Lunar Planet. Sci. Conf. 13th*, Part 1, *J. Geophys. Res.*, *87*, suppl., A159–A170, 1982.

Dickinson, T., G. J. Taylor, K. Keil, R. A. Schmitt, S. S. Hughes, and M. R. Smith, Apollo 14 aluminous mare basalts and their possible relationship to KREEP, *Proc. Lunar Planet. Sci. Conf. 15th*, Part 2, *J. Geophys. Res.*, *90*, suppl., C365–C374, 1985.

Gaddis, L. R., C. M. Pieters, and B. R. Hawke, Remote sensing of lunar pyroclastic glasses, *Icarus*, *61*, 461–489, 1985.

Giguere, T. A., G. J. Taylor, B. R. Hawke, and P. G. Lucey, The titanium contents of lunar mare basalts, *Meteorit. Planet. Sci.*, *35*, 193–200, 2000.

Gillis, J. J., L. A. Haskin, and P. D. Spudis, An empirical calibration to calculate thorium abundance from the Lunar Prospector gamma-ray data, *Lunar Planet. Sci. [CD-ROM], XXX*, abstract 1699, 1999.

Gillis, J. J., B. L. Jolliff, R. L. Korotev, and D. J. Lawrence, An empirical relation between the Lunar Prospector gamma-ray and soil sample Th abundances, *Lunar Planet. Sci. [CD-ROM] XXXI*, abstract 2058, 2000.

Haskin, L. A., The Imbrium impact event and the thorium distribution at the lunar highlands surface, *J. Geophys. Res.*, *103*, 1679–1689, 1998.

Haskin, L. A., R. L. Korotev, K. L. Rockow, and B. L. Jolliff, The case for an Imbrium origin of the Apollo thorium-rich impact-melt breccias, *Meteorit. Planet. Sci.*, *33*, 959–975, 1998.

Hawke, B. R., C. R. Coombs, L. R. Gaddis, P. G. Lucey, and P. D. Owensby, Remote sensing and geologic studies of localized dark mantle deposits on the Moon, *Proc. Lunar Planet. Sci. Conf. 19th*, 255–268, 1989.

Herbert, F., Time-dependent lunar density models, *Proc. Lunar Planet. Sci. Conf. 11th*, 2015-2030, 1980.

Hess, P. C., and E. M., Parmentier, A model for the thermal and chemical evolution of the Moon's interior: Implications for the onset of Mare volcanism, *Earth Planet. Sci. Lett.*, *164*, 501-514, 1995.

Housen, K. R., R. M. Schmitt, and K. A. Holsapple, Crater ejecta scaling laws: Fundamental forms based on dimensional analysis, *J. Geophys. Res.*, *88*, 2485–2499, 1983.

Jolliff, B. L., R. L. Korotev, and L. A. Haskin, Geochemistry of 2–4 mm particles from Apollo 14 soil (14161) and implications regarding igneous components and soil-forming processes, *Proc. Lunar Planet. Sci. Conf. 21st*, 193–219, 1991.

Jolliff, B. L., C. Floss, I. S. McCallum, and J. M. Schwartz, Geochemistry, petrology, and cooling history of 14161,7373: A plutonic lunar sample with textural evidence of granitic-fraction separation by silicate-liquid immiscibility, *Am. Mineral.*, *84*, 821–837, 1999.

Jolliff, B. L., J. J. Gillis, L. A. Haskin, R. L. Korotev, and M. A. Wieczorek, Major lunar crustal terranes: Surface expressions and crust-mantle origins, *J. Geophys. Res.*, *105*, 4197–4216, 2000.

Korotev, R. L., Mixing levels, the Apennine Front soil component, and compositional trends in the Apollo 15 soils, *Proc. Lunar Planet. Sci. Conf. 17th*, Part 2, *J. Geophys. Res.*, *92*, suppl., E411–E431, 1987.

Korotev, R. L., Concentrations of radioactive elements in lunar materials, *J. Geophys. Res.*, *103*, 1691–1701, 1998.

Korotev, R. L., A new estimate of the composition of the feldspathic upper crust of the Moon, *Lunar Planet. Sci. [CD-ROM]. XXX*, abstract 1303, 1999.

Korotev, R. L., The great lunar hot spot and the composition and origin of the Apollo mafic ("LKFM") impact-melt breccias, *J. Geophys. Res.*, *105*, 4317–4345, 2000.

Korotev, R. L., B. L. Jolliff, and R. A. Zeigler, The KREEP components of the Apollo 12 regolith, *Lunar Planet. Sci. [CD-ROM], XXXI*, abstract 1363, 2000.

Lawrence, D. J., W. C. Feldman, B. L. Barraclough, A. B. Binder, R. C. Elphic, S. Maurice, and D. R. Thomsen, Global elemental maps of the

Moon: The Lunar Prospector Gamma-Ray Spectrometer, *Science, 281*, 1484–1489, 1998.

Lawrence, D. J., W. C. Feldman, B. L. Barraclough, R. C. Elphic, S. Maurice, A. B. Binder, M. C. Miller, and T. H. Prettyman, High resolution measurements of absolute thorium abundances on the lunar surface from the Lunar Prospector gamma-ray spectrometer, *Geophys. Res. Lett., 26*, 2681–2684, 1999.

Longhi, J., Fractionation trends of evolved lunar magmas, *Lunar Planet. Sci. XX*, 584–585, 1989.

Lucchitta, B. K., Geologic map of the north side of the Moon, *U.S. Geol. Surv. Map, I-1062*, scale 1:5,000,000, 1978.

Lucey, P. G., D. T. Blewett, and B. R. Hawke, Mapping the FeO and TiO_2 content of the lunar surface with multispectral imagery, *J. Geophys. Res., 103*, 3679–3699, 1998.

Lucey, P. G., D. T. Blewett, and B. L. Jolliff, Lunar iron and titanium abundance algorithms based on final processing of Clementine UVVIS images, *J. Geophys. Res.*, this issue.

McCallum, I. S., and H. E. O'Brien, Stratigraphy of the lunar highland crust: Depths of burial of lunar samples from cooling-rate studies, *Am. Mineral., 81*, 1166–1175, 1996.

Neumann, G. A., M. T. Zuber, D. E. Smith, and F. G. Lemoine, The lunar crust: Global structure and signature of major basins, *J. Geophys. Res., 101*, 16,841–16,863, 1996.

Oberbeck, V. R., The role of ballistic erosion and sedimentation in Lunar stratigraphy, *Rev. Geophys., 13*, 337–362, 1975.

Palme H., B. Spettel, K. P. Jochum, G. Dreibus, H. Weber, G. Weckwerth, H. Wänke, A. Bischoff, and D. Stöffler, Lunar highland meteorites and the composition of the lunar crust, *Geochim. Cosmochim. Acta, 55*, 3105–3122, 1991.

Papike, J. J., G. Ryder, and C. K. Shearer, Lunar samples, in *Rev. Mineral., 36*, 5–1 to 5–234, 1998.

Pieters, C. M., Mare basalt types of the front side of the Moon: A summary of spectral reflectance data, *Proc. Lunar Planet. Sci. Conf. 9th*, 2825–2849, 1978.

Pieters, C. M., J. W. Head, J. B. Adams, T. B. McCord, S. H. Zisk, and J. L. Whitford-Stark, Late high titanium basalts of the western maria: Geology of the Flamstead region of Oceanus Procellarum, *J. Geophys. Res., 85*, 3913–3938, 1980.

Ryder, G., Coincidence in time of the Imbrium basin impact and Apollo 15 KREEP volcanic flows: The case for impact-induced melting, in *Large Meteorite Impacts and Planetary Evolution*, edited by B. O. Dressler, R. A. F. Grieve, and V. L. Sharpton, *Spec. Pap. Geol. Soc. Am., 293*, 11–18, 1994.

Schultz, P. H., and D. E. Gault, Seismically induced modification of lunar surface features, *Proc. Lunar Sci. Conf. 6th*, 2845–2862, 1975.

Shearer, C. K., and J. J. Papike, Basaltic magmatism on the Moon: A perspective from volcanic picritic glass beads, *Geochim. Cosmochim. Acta, 57*, 4785–4812, 1993.

Shervais, J. W., L. A. Taylor, and M. M. Lindstrom, Apollo 14 mare basalts: Petrology and geochemistry of clasts from consortium breccia 14321, *Proc. Lunar Planet. Sci. Conf. 15th*, Part 2, *J. Geophys. Res., 90*, suppl., C375–C395, 1985a.

Shervais, J. W., L. A. Taylor, J. C. Laul, C.-Y. Shih, and L. E. Nyquist, Very high potassium (VHK) basalt: Complications in mare basalt petrogenesis, *Proc. Lunar Planet. Sci. Conf. 16th*, Part 1, *J. Geophys. Res., 90*, suppl., D3–D18, 1985b.

Shih, C.-Y., L. E. Nyquist, D. D. Bogard, B. M. Bansal, H. Wiesmann, P. Johnson, J. W. Shervais, and L. A. Taylor, Geochronology and petrogenesis of Apollo 14 very high potassium mare basalts, *Proc. Lunar Planet. Sci. Conf. 16th*, Part 2, *J. Geophys. Res. 91*, suppl., D214–D228, 1986.

Spudis, P. D., *The Geology of Multi-Ring Impact Basins*, 263 pp., Cambridge Univ. Press, New York, 1993.

Warren, P. H., The origin of pristine KREEP: Effects of mixing between urKREEP and the magmas parental to the Mg-rich cumulates, *Proc. Lunar Planet. Sci. Conf. 18th*, 233-241, 1988.

Whitaker, E. A., The lunar Procellarum basin, in *Multi-ring Basins, Proc. Lunar Planet. Sci. Conf. 12th, Part A*, 105–111, 1981.

Wieczorek, M. A., and R. J. Phillips, The "Procellarum KREEP Terrane": Implications for mare volcanism and lunar evolution, this issue.

Wieczorek, M. A., and R. J. Phillips, Lunar multiring basins and the cratering process, *Icarus, 139*, 246–259, 1999.

Wilhelms, D. E., The Geologic History of the Moon, U. S. Geol. Surv. Pap. 1348, 302 pp., 1987.

Wilhelms, D. E., and J. F. McCauley, Geologic map of the near side of the Moon, *U.S. Geol. Surv. Map, I-703*, scale 1:5,000,000, 1971.

J. J. Gillis, L. A. Haskin, B. L. Jolliff, and R. L. Korotev, Department of Earth and Planetary Sciences, Washington University, Campus Box 1169, One Brookings Dr., St. Louis, MO 63130. (lah@levee.wustl.edu)

(Received June 21, 1999; revised March 13, 2000;
accepted March 23, 2000)